

Serveur Académique Lausannois SERVAL [serval.unil.ch](http://serval.unil.ch)

## Author Manuscript

Faculty of Biology and Medicine Publication

**This paper has been peer-reviewed but does not include the final publisher proof-corrections or journal pagination.**

Published in final edited form as:

**Title:** Coat color dilution in mice because of inactivation of the melanoma antigen MART-1.

**Authors:** Aydin IT, Hummler E, Smit NP, Beermann F

**Journal:** Pigment cell & melanoma research

**Year:** 2012 Jan

**Volume:** 25

**Issue:** 1

**Pages:** 37-46

**DOI:** 10.1111/j.1755-148X.2011.00910.x

In the absence of a copyright statement, users should assume that standard copyright protection applies, unless the article contains an explicit statement to the contrary. In case of doubt, contact the journal publisher to verify the copyright status of an article.

## **Coat color dilution in mice due to inactivation of the melanoma antigen MART-1**

Iraz T. Aydin<sup>1</sup>, Edith Hummler<sup>2</sup>, Nico P.M. Smit<sup>3</sup>, Friedrich Beermann<sup>1\*</sup>

<sup>1</sup> Swiss Institute for Experimental Cancer Research (ISREC), School of Life Sciences, Ecole Polytechnique Fédérale de Lausanne (EPFL), CH-1015 Lausanne, Switzerland

<sup>2</sup> Department of Pharmacology and Toxicology, University of Lausanne, CH-1005 Lausanne, Switzerland

<sup>3</sup> Department of Clinical Chemistry, Leiden University Medical Center, Leiden, The Netherlands

\* CORRESPONDENCE: F. Beermann, e-mail: Friedrich.Beermann@epfl.ch

## Summary

MART-1 is a melanoma-specific antigen, which has been thoroughly studied in the context of immunotherapy against malignant melanoma, and which is found only in the pigment cell lineage. However, its exact function and involvement in pigmentation is not clearly understood. MART-1 has been shown to interact with the melanosomal proteins Pmel17 and OA1. To understand the function of MART-1 in pigmentation, we developed a new knockout mouse model. Mice deficient in MART-1 are viable, but loss of MART-1 leads to a coat color phenotype, with a reduction in total melanin content of the skin and hair. Lack of MART-1 did not affect localization of melanocyte-specific proteins nor maturation of Pmel17. Melanosomes of hair follicle melanocytes in MART-1 knockout mice displayed morphological abnormalities, which were exclusive to stage III and IV melanosomes. In conclusion, our results suggest that MART-1 is a pigmentation gene which is required for melanosome biogenesis and/or maintenance.

## **Significance**

MART-1 is one of the highly cited pigment cell-specific proteins since it has been considered as a good candidate for immunotherapy against malignant melanoma. However, little is known on its biology, regulation and function. Its specific expression in the pigment cell lineage and subcellular localization to melanosomes suggest that it might be involved in pigmentation. Here we addressed this issue and have generated a new knockout mouse model. Our study showed that MART-1 loss led to a coat color phenotype, reduced melanin production and aberrant melanosomes.

**Keywords:** Knockout, MART-1, Melan-A, mlana, melanocytes, melanosome, pigment

**Running Title:** Analysis of a MART-1 knockout

## **Introduction**

Pigment-producing cells are responsible for the color variation of organisms. In lower vertebrates, this can be exerted by chromatophores, xanthophores and melanophores, whereas in mammals solely melanocytes are responsible for providing skin color. Apart from producing the melanin pigment and therefore providing pigment granules to skin and hair, melanocytes serve several other functions and are implicated in protection against UV damage, hearing function, inflammation, and reduction and binding of reactive oxygen species (Plonka et al., 2009).

Pigmentation is a complex process that requires the involvement of almost 400 loci (Montoliu et al., 2011). Some of these loci code for pigment cell-specific genes, which are specifically located in the melanosomes. Such melanosomal proteins as the tyrosinase gene family members (tyrosinase, TYRP1, DCT), Pmel17, OA1 or MART-1 are involved either in melanosome biogenesis or production of the melanin pigment. Melanosomes are organelles which are specific for pigment cells. They originate from early endosomes and mature through four morphologically distinct stages. Stage I melanosomes contain the intraluminal vesicles (ILVs) carrying Pmel17. At stage II fibril formation starts and, by stage III, the melanosomal proteins are trafficked to the melanosomes and the pigment synthesis begins. The stage IV melanosomes are fully pigmented and, in skin melanocytes, move towards the dendrites to be transferred to the keratinocytes (Raposo and Marks, 2007). The timing and progress of melanosome biogenesis depend on proper trafficking and processing of the melanosomal proteins. Some of the melanosomal proteins as tyrosinase or DCT have defined functions in melanogenesis, however the involvement of OA1, MART-1 and p in melanogenesis is not completely understood.

In 1994, as a result of the search for melanoma antigens, two groups independently cloned a new gene, named *MART-1/Melan-A/mlana* (hereafter: MART-1), which encodes a melanoma antigen recognized by cytotoxic T lymphocytes (Coulie et al., 1994; Kawakami et al., 1994). The discovery of such melanoma antigens has been promising for developing peptide vaccines to generate an immune response against melanoma cells (Coulie et al., 1994; Kawakami et al., 1994). Expression of MART-1 is limited to melanocytes, melanomas and the RPE (Aydin and Beermann, 2009; Kawakami et al., 1994). The *MART-1* gene encodes a single-pass membrane protein, which is located mainly in the endoplasmic reticulum, trans-Golgi network and melanosomes, and here in particular to early melanosomes. MART-1 has a short half-life, it is ubiquitylated and is targeted from melanosomes to lysosomes for degradation (Basrur et al., 2003; De Maziere et al., 2002; Kawakami et al., 1997; Levy et al., 2005; Rimoldi et al., 2001).

Even though MART-1 has been widely studied in the context of melanoma immunotherapy, the information regarding its function in pigment cells is very limited. Nevertheless, the high enrichment of MART-1 in early melanosomes suggested that it might play a role in early melanogenesis. In 2005, Hoashi *et al* (Hoashi et al., 2005) published a report providing first results on a possible function of MART-1. They showed that, in human melanoma cells, MART-1 physically interacts with the melanosomal protein Pmel17, and depletion of MART-1 by siRNA led to defects in stability, processing and trafficking of Pmel17. Re-expression of MART-1 in WM266-4 human melanoma cells lacking MART-1 expression led to Pmel17 upregulation and formation of striated fibrils, which are very few in WM266-4 cells (Hoashi et al., 2005). More recently, it was reported that MART-1 interacts directly with the melanosomal protein OA1 (Giordano et al., 2009). Upon MART-1 depletion by siRNA, OA1 protein levels were reduced and its subcellular distribution was affected. The cells devoid in MART-1 had many aberrant enlarged compartments which contained abnormally

large intraluminal vesicles (ILVs). Even though Pmel17 processing seemed to be affected, an effect on Pmel17 trafficking could not be confirmed (Giordano et al., 2009; Hoashi et al., 2005). Their data led to the suggestion that MART-1 might have a function in transport and stabilization of OA1 and thus might act as an escort protein. Since MART-1 is exclusively expressed in pigment cells and it is abundantly found in early melanosomes, it might indeed play a role in melanosome biogenesis.

These published works on MART-1 function have been performed using melanocyte and melanoma cells. However, a genetic approach to MART-1 function was not realized until now, and it remained an open question whether MART-1 would be required in mouse pigmentation. To address this issue, we followed a different approach from the previous studies and genetically inactivated the MART-1 gene by gene targeting in embryonic stem (ES) cells and have generated a novel mouse model lacking MART-1. Our data provide evidence that MART-1 is a pigmentation gene which leads to a coat color phenotype in MART-1 knockout mice.

## **Results**

### **Generation of MART-1 knockout mice**

The *MART-1* gene comprises 5 exons, with the translation start site located in the second exon, and the second and third exons encoding the transmembrane domain (Rimoldi et al., 2001) (Figure 1A). To eliminate the function of MART-1 we therefore targeted and removed exons 2 (containing the ATG) and 3. We did not remove the first exon, since it is untranslated and thus not yields a truncated protein. The targeting construct contained loxP sites flanking the second and third exon, as well as the selection cassette P<sub>gk</sub>-neo flanked by frt sites

(Figure 1A). The targeting construct was linearized and electroporated into mouse embryonic stem (ES) cells from 129/SvEv mice, the correctly recombined clones were detected by PCR and Southern blot analysis (Figure 1B). 7 out of 480 ES cell clones showed correct recombination. One of the clones was then used for blastocyst injection (Porret et al., 2006), and 2 chimeric males transmitted the *MART-1<sup>lox-neo</sup>* allele through the germline. Successive rounds of mating to *hACTB::FLP* mice (Dymecki, 1996) and to *Nestin::Cre* mice (Dubois et al., 2006) allowed to remove the P<sub>gk</sub>-neo cassette (resulting in *MART-1<sup>fl/+</sup>* mice, Figure 1C) and to generate a constitutive *MART-1* knockout (*MART-1<sup>-</sup>*) allele. In further rounds of matings, the transgenes *hACTB::FLP* and *Nestin::Cre* were eliminated from mice carrying the *MART-1<sup>+/-</sup>* genotype. Mating of *MART-1<sup>+/-</sup>* mice resulted in *MART-1<sup>-/-</sup>* mice (Figure 1C, G), in accordance with the expected Mendelian ratio (*MART-1<sup>+/+</sup>*: 23.3%, *MART-1<sup>+/-</sup>*: 50.3%, *MART-1<sup>-/-</sup>*: 26.4%, n=360). RT-PCR on skin samples of *MART-1<sup>-/-</sup>* mice confirmed absence of *MART-1* mRNA while tyrosinase mRNA and Dct mRNA were detected (Figure 1D). We then used an antibody recognizing the C terminus of *MART-1* which is encoded by sequences not deleted in the mice. No *MART-1* protein was detected in melanocytes isolated from the trunk of newborn *MART-1<sup>-/-</sup>* mice (Figure 1E, F), and these results altogether confirmed the generation of a knockout of *MART-1*.

### **Loss of *MART-1* leads to a coat color dilution**

*MART-1<sup>-/-</sup>* mice displayed a dilution of the coat color (Figure 1G), visible at 5 days after birth. The coat color phenotype was not progressive, and it was visible throughout the life of the mice. *MART-1<sup>+/-</sup>* mice did not have any coat color phenotype (not shown). This remained the only visible effect of *MART-1* deletion and such *MART-1<sup>-/-</sup>* mice did not display any problems of growth or fertility. A dilution in the color was not visible in other pigmented

tissues such as tail skin or footpads. Histological analysis of heart, lung, kidney, liver, thymus, spleen, pancreas, gallbladder, brain, stomach, small intestine, colon, prostate, testis, tongue, skin, eyes and spinal column did not reveal any abnormalities (not shown).

In order to evaluate the coat color phenotype, melanin content of hair samples was determined, revealing a 25% reduction in hairs from knockout mice (Figure 2A). For a more precise analysis, the eumelanin content of skin samples from 1 month-old *MART-1*<sup>+/+</sup> and *MART-1*<sup>-/-</sup> mice was measured by HPLC. The reduction in the eumelanin content of the *MART-1*<sup>-/-</sup> skin confirmed the reduction observed in hair melanin content (Figure 2B), and was thus in accordance with the visible phenotype. Preliminary HPLC measurements of pheomelanin did not yield reliable values, and we can therefore not exclude that pheomelanin might be differently affected. The results nevertheless indicate that the observed coat color phenotype is due to a reduction in melanin.

### **Loss of MART-1 does not affect other melanosomal proteins**

The results on melanin production suggested a possible effect on melanogenesis. It has been shown previously that down-regulation of MART-1 in human melanoma cells affects the processing and trafficking of the melanosomal protein Pmel17 (Hoashi et al., 2005). We therefore investigated the localization and processing of proteins that are important for melanosome biogenesis and melanin biosynthesis.

We first performed immunostaining of skin sections of P6 (not shown) and P30 (Figure 3) mice, and, here, neither distribution of Pmel17 nor of other melanosomal proteins as tyrosinase, Tyrp1, and Dct seemed to be affected by MART-1 loss. Hoashi *et al* (2005) had reported that, upon MART-1 depletion, human melanoma cells displayed aberrant processing

of Pmel17. We therefore asked whether this is true for MART-1-deficient mouse melanocytes. Since skin extracts would not allow to reveal sufficient levels of melanocyte proteins, we established melanocyte cultures from newborn *MART-1<sup>+/+</sup>* and *MART-1<sup>-/-</sup>* mice. Immunofluorescence for melanocyte proteins corroborated the origin of the cultures (not shown), and they were either expressing (*MART-1<sup>+/+</sup>*) or lacking MART-1 (*MART-1<sup>-/-</sup>*) (Figure 1E, F). In addition, the immunofluorescence stainings and detailed confocal analysis (Figure S1) on these established cell lines did not reveal any changes in protein localization upon MART-1 loss. During melanosome biogenesis, Pmel17 normally undergoes a series of proteolytic cleavages. First, the immature P1 form is processed and the interim P2 form is produced, which is then cleaved by a proprotein convertase. M $\alpha$  and M $\beta$  fragments are formed, and M $\alpha$  is further cleaved into M $\alpha$ N and M $\alpha$ C fragments. The  $\alpha$ Pep13h antibody recognizes the C terminus of the protein, and allows to detect both P1 and M $\beta$  forms (Figure 4D) (Berson et al., 2001; Kummer et al., 2009). Western blot analysis against Pmel17 using the  $\alpha$ Pep13h antibody nevertheless revealed that, in *MART-1<sup>-/-</sup>* melanocytes, Pmel17 was successfully cleaved and the M $\beta$  fragment was produced (Figure 4A). Additionally, using the HMB45 antibody recognizing the M $\alpha$  and M $\alpha$ C fragments (Figure 4D), mature M $\alpha$ C fragments were detected in *MART-1<sup>-/-</sup>* melanocytes (Figure 4B), and in particular found in the insoluble protein fraction (Figure 4C). Due to rapid degradation, it was not possible to visualize the C-terminal fragment (CTF) of Pmel17 (Hoashi et al., 2006; Theos et al., 2005). These results altogether suggest that neither the localization nor the expression of Pmel17 and the members of the tyrosinase gene family were affected by loss of MART-1 in mouse melanocytes.

### **Loss of MART-1 affects the melanosome morphology**

Defects or depletion of pigment-cell specific genes such as *Dct* (14), *Pmel17* (34, 35), and *OAI* (8, 13), or genes encoding the subunits of cargo proteins involved in melanosomal protein trafficking such as *Cno*, *Hps3*, *Hps5*, *Hps6*, *Bloc1s3* or *Ap3b1* (26) are known to affect melanosome morphology. In order to detect the effect of MART-1 deficiency on melanosome morphology, we examined the ultrastructure of hair follicle melanocytes, knowing that they are providing the visible coat color phenotype. Bulb regions of anagen hair follicles from 1 month-old *MART-1<sup>+/+</sup>* and *MART-1<sup>-/-</sup>* littermates were examined under a transmission electron microscope (TEM). Visual inspection of sections revealed no obvious change in number and size of melanosomes, even though we cannot include some minor effects. In contrast, the sections clearly revealed that MART-1 loss was indeed affecting melanosome structure. Different from the melanosomes of *MART-1<sup>+/+</sup>* littermates (Figure 5A), the melanosomes of *MART-1<sup>-/-</sup>* mice (Figure 5B, C) displayed blebbing of the limiting membrane and vesicles were observed between the pigmented compartment and the limiting membrane. Some of the stage IV melanosomes in the MART-1 knockout skin had a gap between the pigmented compartment and the limiting membrane and some vesicles were observed in this space (Figure 5D-G). In contrast, such structures were not seen in melanosomes from wildtype mice (Figure 5A). Interestingly, loss of MART-1 did not affect the morphology of the melanosomes located in the RPE (Figure S2). There is very little or no melanin turnover in adult eyes (Schraermeyer, 1993; Schraermeyer et al., 2006), and, at the time of melanosome biogenesis during embryonic development, MART-1 expression seems rather low. This might explain the lack of a visible melanosome morphology phenotype in the eyes of MART-1 knockout mice.

The affected melanosomes were of the stages III and IV, and stage I and II melanosomes seemed to be unaffected. To further confirm this we analyzed the ultrastructure of hair follicle melanocytes of albino mice which lack stage III and IV melanosomes. Albino (*Tyr<sup>c</sup>*)

*MART-1*<sup>-/-</sup> mice were obtained following mating to FVB/N mice. Electron micrographs confirmed the presence of unaffected stage I and II melanosomes (Figure 5I). This confirms, that the absence of MART-1 is affecting stage III and stage IV melanosomes.

## **Discussion**

Since its identification and cloning in 1994, MART-1 has been one of the most studied proteins in melanoma immunotherapy, even though nearly nothing is known on MART-1 function (Coulie et al., 1994; Kawakami et al., 1994). Since MART-1 is exclusively located in melanosomes of pigment cells, it was considered to be involved in melanogenesis. Previous results in human melanoma cells have suggested that MART-1 is required for trafficking and processing of Pmel17 (Hoashi et al., 2005). More recently, another study showed that MART-1 depletion causes a reduction of OA1 protein levels due to rapid lysosomal degradation and thus affects its subcellular distribution (Giordano et al., 2009). Here, we report the generation of a new knockout mouse model, which contributes to elucidating the function of MART-1 in the pigmented system. Upon MART-1 deletion we observed a coat color phenotype and a reduction in total melanin content, which is most probably caused by abnormal melanosome morphology.

Previously, it has been reported that MART-1 is involved in Pmel17 processing and trafficking (Hoashi et al., 2005). Downregulation of human MART-1 affected subcellular distribution and processing of Pmel17 and therefore reduced the formation of mature M $\alpha$ C fragments. However, these experiments were performed essentially with human melanocytes and melanoma cells, and MART-1 was silenced and not absent (Hoashi et al., 2005). We thus analyzed Pmel17 processing in melanocyte cell lines established from MART-1 knockout mice (Figure 4). Surprisingly, Pmel17 was normally processed and the M $\alpha$ C fragments were

produced similarly in knockout and wildtype mouse melanocytes. This difference might be due to the silencing approach, since it can never completely be excluded that other genes besides *MART-1* are affected. In addition, the kinetics of Pmel17 processing in mouse and human melanocytes differs (Theos et al., 2006). In mice, Pmel17 processing is very rapid and most of the intermediate processing products observed in human melanocytes are not seen in the mouse. Processing of Pmel17 leading to fibril formation could therefore be different in mouse and human, and Pmel17 processing might be independent of MART-1 in mice, and hence not different in the MART-1 knockout melanocyte. We would equally like to emphasize at this point that we did not aim to address the trafficking and the biochemistry of the melanosomes as in the published in vitro work, and can thus not completely exclude any differences due to the methods used. Recently, MART-1 was reported to be required for stability of OA1 (Giordano et al., 2009). Unfortunately, we were not able to monitor any changes in OA1 (not shown), most likely due to the failure of the antibody to unequivocally recognizing the mouse OA1 protein.

When electron micrographs of hair follicle melanocytes of pigmented mice were analyzed, melanosome biogenesis seemed normal at early stages. This was confirmed by analyzing hair follicle melanocytes of albino (*Tyr<sup>c</sup>*) wildtype and MART-1 knockout mice, where no stage III and IV melanosomes are present. However, morphological defects became apparent when stage III and stage IV melanosomes of pigmented MART-1 knockout and wildtype hair follicle melanocytes were compared, showing for example blebbing of the limiting membrane of the melanosome (Figure 5C-G). A similar melanosomal phenotype has been observed in melanocytes of the pearl (*Ap3b1<sup>pe</sup>*) mice, which are a model for Hermansky-Pudlak syndrome (HPS) (Nguyen et al., 2002). Nevertheless, MART-1 seems to be an unlikely candidate for HPS, since MART-1 expression is restricted to the pigment cell lineage, whereas HPS is a multiple-system disease affecting the lysosome related organelles from many different cell

types (Huizing et al., 2000). A link to HPS had equally been suggested due to the chromosomal localization of *MART-1* next to identified coat color mutations of the *HPS6* gene. However, this has been subsequently ruled out by chromosomal in situ hybridization (Wright et al., 1997).

The vesicles we observed in late stage melanosomes of *MART-1*<sup>-/-</sup> mice (Figure 5D-F) resemble autophagic vesicles. It might thus be possible that MART-1 loss triggers a chain of events that leads to melanosome autophagy. In this case the melanosomes would be lysed before and/or after being transferred to the neighboring keratinocytes. This would lead to a significant reduction in the number of healthy melanosomes successfully transferred to keratinocytes and due to the reduced number of melanosomes received by keratinocytes a reduction in total melanin content of hair and skin could be explained. This theory is also supported by several studies showing the involvement of autophagic processes in order to eliminate defective melanosomes (Boissy et al., 1986; Bomirski et al., 1987; Ho and Ganesan, 2011; Lazova et al., 2010; Lazova and Pawelek, 2009; Smith et al., 2005). The effect of MART-1 loss on melanosome numbers was not obvious. Nevertheless, we cannot exclude at this point that melanin synthesis is less efficient in such malformed melanosomes and might thus at least partially contribute to a lower melanin level.

In the melanosome, MART-1 is located on the limiting membrane (De Maziere et al., 2002), and has no domains that would suggest an enzymatic role. Previous studies (Giordano et al., 2009; Hoashi et al., 2005) showed that MART-1 might be involved in trafficking of melanosomal proteins. We observed an irregular membrane structure of the melanosomes of MART-1 knockout mice, which could be due to abnormal or increased fusion of transport vesicles. This observation indicates that MART-1 might play a role in vesicular trafficking.

There are no known *MART-1* gene mutations and it has not been associated with any pigmentation disorders in humans, mice or zebrafish which might be explained partly by the small size of the gene. In addition, the expected effect of loss of MART-1 would only lead to a 25% reduction in total melanin content (Figure 2), and putative point mutations might not lead to loss-of-function alleles. Thus, it would be difficult to detect a small reduction considering the variation of skin and hair color in humans. In conclusion, our results show that MART-1 affects melanosome morphology by a yet unidentified mechanism. Whereas deficiency of MART-1 is compatible with life, our results are consistent with an expression of MART-1 only in the pigment cell lineage, confirming that it is an appropriate target for melanoma therapy. Moreover, our results add MART-1 to the growing list of genes affecting coat color in mice.

## **Methods**

### **Generation of the targeting vector and the knockout mice**

The targeting vector was constructed in separate steps (Rubera et al., 2002). The amplicons were amplified using a BAC clone (bMQ-318G24) (from 129S7/SvEv mice) as a template (Adams et al., 2005). First, the C1 plasmid was prepared by cloning the 5' homologous arm (*ApaI/XhoI* fragment, exon 1 and intron 1, amplified with primers MKO\_5F: AAAGGGCCC ATATGACATACAGAGCCAGACAGCA, MKO\_5R: AAAGGGCCC CTAAAGGAAGGGCACATAGGGATT) into K13pATRTneolox antisense (Trumpf et al., 2001). Then C2 was constructed by cloning the 3' homologous arm (*HindIII* fragment, from intron 3 to the end of exon 5, amplified with primers MKO3F: AAAAAGCTT GTGGGTAATGGTCCCCTGAAG, MKO3R: AAAAAGCTT AATATACATTGAGATGTTTATTG) into lox-targeting vector neo/Tk (Radtke et al., 1999).

The third construct, C3, was prepared by cloning the MART-1 vital region (*NotI/AscI* fragment, from exon 2 to the end of exon 3, amplified with primers MKO\_VF: AAA GCGGCCGCGTGTTCAGAGCCTGAACTAATCTGA, MKO\_VR: AAAGGCGCGCC CACGAGATAGGAGAGAACCAACTC) into C2. The final targeting construct was prepared by cloning the MKO5-frt-Neo-frt-lox cassette (*KpnI*(blunt)/*NotI* fragment) from C1 into C3. The targeting construct was sequenced and no mutations were found. In order to control the loxP sites, the targeting vector was transformed into 294-Cre *E.coli* cells (Buchholz et al., 1996) and a successful recombination was observed. The frt sites were tested by electroporating the targeting vector into EL250 *E.coli* cells (Lee et al., 2001). The construct was linearized and electroporated into mouse embryonic stem (ES) cells originated from 129/SvEv mice (Porret et al., 2006).

After selection with G418 and Ganciclovir, 480 ES cell clones were obtained. The recombination was tested by PCR on genomic DNA extracts from ES cells. 5' recombination was confirmed by PCR using the primers ES\_5F: GGTAGAATGAAGTTGGTTTCTTTCA, 5R: GAGACTAGTGAGACGTGCTACTTCC. 3' recombination was confirmed by PCR using the primers ES\_3F: CGCCATAACTTCGTATAGCATAACAT, ES\_3R1: AATTAATTGCATTACTGCCAGAC, ES\_3R2: GAGGATGGTTTTCTCCTCCTG. After confirmation of recombination by Southern blot analysis, one of the correctly recombined clones was selected, injected into 129/SvEv donor blastocysts and male chimeras that transmitted the targeted allele through the germline were obtained.

### **Southern blot analysis**

20µg of ES cell DNA was digested overnight with *Bam*HI, and subjected to Southern blot analysis. Briefly, digested DNA was separated on a 0.8% agarose gel, transferred onto a Hybond N+ membrane and hybridized with  $\alpha$ P32-labeled DNA probes. A *MART-1* probe

(1.6kb, isolated from 2.5::*luc* (Aydin and Beermann, 2009) by *NcoI* digestion) or a Neomycin probe (Merillat et al., 2009) were used for detection. The *MART-1* probe allowed to distinguish the wildtype (13.9 kb) and recombined (9.5 kb) alleles, and correct insertion of P<sub>gk</sub>-neo was confirmed with the Neomycin probe.

### **Mouse care and genotype analysis**

The mouse colonies were maintained in the animal facility of the EPFL. All mouse work has been performed under authorization of cantonal authorities and was conducted according to Swiss guidelines. After breeding, the pups were weaned at P21 and ear biopsies were taken for genotype analysis. For genomic DNA extraction, ear biopsies were lysed in 300µl 50mM NaOH for 10 minutes at 95°C. Then 25µl 1M Tris-HCl (pH 8) were added, samples were vortexed and centrifuged at 12000xg at room temperature for 6 minutes. The supernatant was used for genotyping by PCR. For genotype analysis of the mice the following primers were used: *MART-1* knockout (F1: ATCAAGCTGAAGGCCAGAGA, F2: CGAAGTGGATACAGA ACCTTGA, R: CACCCAGACTGACAAGCTGA), p16 knockout (1: TCCCTCTACTTTTTCTTCTGAC, 2: CGGAACGCAAATATCGCAC, 3: CTAGTGAGACGTGCTACTTC) (Lavado et al., 2005), *Nestin::Cre* (F: CTTGGCTTTGTACTTTCTGTGACTG, R: CCTCCATCCCAGACAAATACATTA C), *hACTB::FLP* (F: GTGGATCGATCCTACCCCTTGCG, R: GGTCCAACACTGCAGCCCAAGCTT).

### **RNA extraction, cDNA synthesis, RT-PCR**

For RNA extraction the TRIzol reagent (Invitrogen) was used. Frozen tissue samples (100mg) were pulverized in a mortar in liquid nitrogen, and the tissue powder was homogenized in 1ml TRIzol. For further steps, the manufacturer's protocol was followed. The RNA concentration was spectrophotometrically measured and the quality of the samples

was assessed by gel electrophoresis. cDNA synthesis was performed using RevertAid H Minus First Strand cDNA synthesis kit (Fermentas). 3µg of RNA was used for each reaction, following the recommended protocol of the manufacturer. cDNA samples were used as a template for RT-PCR analysis. The following primers were used for the RT-PCR reactions (Aydin and Beermann, 2011): *MART-1*: F, ATTGCTCTGCTTATCGGCTGCT, R, CACCATTCTCCAATATCCCTCT; *tyrosinase*: F, AAGTTTACCCAGAAGCCAATG, R, CTGTGGTAGTCGTCTTTGTC; *Dct*; F: AGCAGTATGGCTGGAGCACT, R: AGCCCTTTCCTCTCCTCTCA, *GAPDH*: F, CAAGGTCATCCATGACAACCTTTG, R, GTCCACCACCCTGTTGCTGTAG.

### **Isolation of melanocytes from dorsal skin**

In order to establish immortal melanocyte cell lines, MART-1 knockout mice were mated to *Ink4a-Arf*<sup>-/-</sup> mice that have been backcrossed to C57BL6/N mice for >10 generations (Sviderskaya et al., 2002). Newborn mice (24-36 hours) were used for the protocol developed by Sviderskaya *et al* (1997). Briefly, the day before isolation, XB2 mouse keratinocyte feeder cells were treated with Mitomycin C (Sigma). Dorsal skin was incubated in 0.5% Trypsin (Invitrogen) at 37°C for 1 hour. After trypsinization, the epidermis was separated carefully and minced in 0.025% Trypsin. In order to prevent fibroblast contamination, only the epidermis was used. The minced epidermis was then seeded on XB2 feeder cells in RPMI 1640 containing GlutaMax I (Gibco) supplemented with 5 µg/ml soybean trypsin inhibitor, 10% FCS (not inactivated), 200pM cholera toxin and 200nM TPA. The cells were maintained at 37°C in a 10% CO<sub>2</sub> incubator. After isolation, the medium was changed every 3 days. On day 10-12, cells were harvested for the first time and reseeded on Mitomycin C-treated XB2 cells. Once the culture was confluent, cells were harvested, counted and passaged. For the first 2-4 passages they were seeded on XB2 cells, thereafter they were weaned off the

feeders. Before Western blot and immunostaining experiments, cells were passaged at least 4 times without XB2 feeders.

### **Immunofluorescence staining of skin sections**

Skin samples were fixed in 4% PFA for 2-3 hours, and then dehydrated and embedded in paraffin. For immunostaining, 4 $\mu$ m sections were cut, deparaffinized and rehydrated. For antigen retrieval, sections were boiled for 25 minutes in Tris-EDTA (pH 9.0), and subsequently blocked in blocking buffer (1% serum / 2% BSA / 0.05% Tween) for 1 hour at room temperature. Primary antibodies were diluted in blocking buffer, and sections were incubated with primary antibodies at 4°C overnight. The sections were washed 3 times with PBS and incubated with secondary antibodies diluted in blocking buffer for 1 hour at room temperature. They were then washed and stained with DAPI, and again washed and mounted. The staining was observed under Zeiss AxioPlan (20X objective). Primary antibodies were as follows: rabbit anti-MART-1 (De Maziere et al., 2002; Kawakami et al., 1997) (provided by D. Rimoldi), rabbit anti-Tyrosinase ( $\alpha$ Pep7) (Jimenez et al., 1991), rabbit anti-Tyrp1 ( $\alpha$ Pep1) (Jimenez et al., 1988), rabbit anti-Dct ( $\alpha$ Pep8) (Tsukamoto et al., 1992) (all provided by V. Hearing), mouse anti-HMB45 (Santa Cruz Biotechnology), rabbit anti-Pmel17 ( $\alpha$ Pep13h, provided by M.S. Marks (Berson et al., 2001)), rat anti-LAMP2 (Developmental Studies Hybridoma Bank).

### **Immunofluorescence staining of cultured mouse melanocytes**

For immunostaining, cells were grown for two days in FlexiPerm chambers (Sigma) mounted on glass slides coated with 0.0001% fibronectin. For the staining, the protocol used by Giordano *et al.* was followed (Giordano et al., 2009). Cells were washed with PBS at 37°C, and all the following steps were performed at room temperature. Cells were fixed with 4% PFA for 10 minutes, washed with PBS and quenched for 10 minutes with 50mM glycine and

then saturated with blocking buffer (BB, 1mg/ml BSA in PBS) for 5 minutes. Then cells were permeabilized in incubation buffer (IB, 0.05% saponin, 1mg/ml BSA in PBS) for 30-60 minutes, and then incubated with primary antibodies diluted in IB for 45-60 minutes. Cells were washed 3 times with IB. They were incubated with secondary antibody diluted in IB for 45-60 minutes, then washed once with IB and stained with DAPI, and washed twice with IB and once with BB, and then mounted. Samples were examined with Zeiss LSM 700 confocal laser scanning microscope.

### **Measurement of hair and skin melanin content**

Hair samples were collected from 4 week-old *MART-1<sup>+/+</sup>* and *MART-1<sup>-/-</sup>* mice. Melanin was extracted from 1mg of hair by alkali treatment in 1ml 1M NaOH at 85°C for 4 hours. The optical density of the samples was measured at a wavelength of 475nm. The measurements were performed in duplicates.

The skin samples from 1 month-old *MART-1<sup>+/+</sup>* (n=2) and *MART-1<sup>-/-</sup>* mice (n=2) were frozen in liquid nitrogen in small buckets of a micro-dismembrator and powdered by shaking the small buckets in three sessions. Eumelanin measurements were performed as originally described by Ito and Fujita (Ito and Fujita, 1985) with modifications (Alaluf et al., 2001). The samples were treated in a total reaction volume of 1 ml 0.86 M KCO<sub>3</sub> by the addition of 40 µl 9% H<sub>2</sub>O<sub>2</sub>. Then the tubes were heated in a Dri-Block for 20 min at 100°C. After cooling the samples the reaction was stopped by addition of 20 µl 10% Na<sub>2</sub>SO<sub>3</sub>. The samples were then extracted on a 1cc Oasis WAX cartridge (Waters, MA, USA) according to the instructions of the manufacturer. Briefly, the column was washed with 1 ml methanol, 1 ml dH<sub>2</sub>O. Then 1 ml sample was applied (0.5 ml sample mixed with 0.5 ml 4% phosphoric acid), washed once with 1 ml 2% formic acid and once with 1 ml methanol. The samples were then eluted with 1.5 ml 5% NH<sub>4</sub>OH in acetonitril:isopropanol (40:60) and dried under N<sub>2</sub> (gas) flow at 40°C.

100 µl of the elution buffer was added to the dried sample and the sample was injected to the HPLC system.

### **Electron microscopy**

Mice were anesthetized and fixation was carried out by cardiac perfusion of the fixative (2% paraformaldehyde/2.5% glutaraldehyde in 0.1M phosphate buffer pH 7.4) for 1 hour at room temperature. Skin samples were embedded in 5% agarose and 140µm sections were cut and fixed for 1 hour. After this fixation the samples were washed 3 times (5 minutes) in 0.1M cacodylate buffer, followed by an incubation in 1% osmium tetroxide for 40 minutes, and washed in ddH<sub>2</sub>O. The samples were stained in 1% uranyl acetate, dehydrated in a graded alcohol series, and embedded in Durcupan. 50 nm sections were taken on coated grids, which were contrasted in 1% uranyl for 10 minutes and 0.3% lead citrate for 5 minutes. The grids were imaged under Philips CM-10 transmission electron microscope.

### **Acknowledgements**

Thanks are due to Anne-Marie Mérillat and Andrée Porret of the transgenic animal facility of the University and the University Hospitals of Lausanne for help with generation of the MART-1 knockout mice, to Michelle Blom for help with mouse matings and genotyping, to Graham Knott, Stéphanie Rosset, and Marie Croisier for help with electron microscopy, to Nicolo Riggi for performing pathological analysis, to Mickey Marks, Donata Rimoldi, Vince Hearing and the Developmental Studies Hybridoma Bank at the University of Iowa for providing antibodies, to Donata Rimoldi for support and discussion, to Manuel Serrano for *Ink4a*<sup>-/-</sup> mice and to Dot Bennett and Elena Sviderskaya of the Wellcome Trust Functional Genomics Cell Bank for protocols and cells. The work was supported by grants from

Oncosuisse (to FB), the Fondation Emma Muschamps (to FB) and The Swiss National Science Foundation (to FB and EH).

### **Supporting information**

Additional Supporting Information may be found in the online version of this article.

**Figure S1** Distribution of Tyrp1 and Pmel17 in wildtype and knockout melanocytes

**Figure S2** Melanosomes in RPE of wildtype and knockout mice

**Appendix** Supplementary Figure legends

## References

- Adams, D. J., Quail, M. A., Cox, T., Van Der Weyden, L., Gorick, B. D., Su, Q., Chan, W. I., Davies, R., Bonfield, J. K., Law, F., et al. (2005). A genome-wide, end-sequenced 129Sv BAC library resource for targeting vector construction. *Genomics* 86, 753-8.
- Alaluf, S., Heath, A., Carter, N., Atkins, D., Mahalingam, H., Barrett, K., Kolb, R., and Smit, N. (2001). Variation in melanin content and composition in type V and VI photoexposed and photoprotected human skin: the dominant role of DHI. *Pigment Cell Res* 14, 337-47.
- Aydin, I. T., and Beermann, F. (2009). Melanocyte and RPE-specific expression in transgenic mice by mouse MART-1/Melan-A/mlana regulatory sequences. *Pigment Cell Melanoma Res* 22, 854-6.
- Aydin, I. T., and Beermann, F. (2011). A MART-1::Cre transgenic line induces recombination in melanocytes and RPE. *Genesis* doi:10.1002/dvg.20725.
- Basrur, V., Yang, F., Kushimoto, T., Higashimoto, Y., Yasumoto, K., Valencia, J., Muller, J., Vieira, W. D., Watabe, H., Shabanowitz, J., et al. (2003). Proteomic analysis of early melanosomes: identification of novel melanosomal proteins. *J Proteome Res* 2, 69-79.
- Berson, J. F., Harper, D. C., Tenza, D., Raposo, G., and Marks, M. S. (2001). Pmel17 initiates premelanosome morphogenesis within multivesicular bodies. *Mol Biol Cell* 12, 3451-64.
- Boissy, R. E., Moellmann, G., Trainer, A. T., Smyth, J. R., Jr., and Lerner, A. B. (1986). Delayed-amelanotic (DAM or Smyth) chicken: melanocyte dysfunction in vivo and in vitro. *J Invest Dermatol* 86, 149-56.
- Bomirski, A., Wrzolkowa, T., Arendarczyk, M., Bomirska, M., Kuklinska, E., Slominski, A., and Moellmann, G. (1987). Pathology and ultrastructural characteristics of a

- hypomelanotic variant of transplantable hamster melanoma with elevated tyrosinase activity. *J Invest Dermatol* 89, 469-73.
- Buchholz, F., Angrand, P. O., and Stewart, A. F. (1996). A simple assay to determine the functionality of Cre or FLP recombination targets in genomic manipulation constructs. *Nucleic Acids Res* 24, 3118-9.
- Coulie, P. G., Brichard, V., Van, P. A., Wolfel, T., Schneider, J., Traversari, C., Mattei, S., De, P. E., Lurquin, C., Szikora, J. P., et al. (1994). A new gene coding for a differentiation antigen recognized by autologous cytolytic T lymphocytes on HLA-A2 melanomas. *J Exp Med* 180, 35-42.
- De Maziere, A. M., Muehlethaler, K., Van, D. E., Salvi, S., Davoust, J., Cerottini, J. C., Levy, F., Slot, J. W., and Rimoldi, D. (2002). The melanocytic protein Melan-A/MART-1 has a subcellular localization distinct from typical melanosomal proteins. *Traffic* 3, 678-693.
- Dubois, N. C., Hofmann, D., Kaloulis, K., Bishop, J. M., and Trumpp, A. (2006). Nestin-Cre transgenic mouse line Nes-Cre1 mediates highly efficient Cre/loxP mediated recombination in the nervous system, kidney, and somite-derived tissues. *Genesis* 44, 355-60.
- Dymecki, S. M. (1996). Flp recombinase promotes site-specific DNA recombination in embryonic stem cells and transgenic mice. *Proc Natl Acad Sci U S A* 93, 6191-6.
- Giordano, F., Bonetti, C., Surace, E. M., Marigo, V., and Raposo, G. (2009). The ocular albinism type 1 (OA1) G-protein-coupled receptor functions with MART-1 at early stages of melanogenesis to control melanosome identity and composition. *Hum Mol Genet* 18, 4530-4545.
- Ho, H., and Ganesan, A. K. (2011). The pleiotropic roles of autophagy regulators in melanogenesis. *Pigment Cell Melanoma Res* 24, 595-604.

- Hoashi, T., Muller, J., Vieira, W. D., Rouzaud, F., Kikuchi, K., Tamaki, K., and Hearing, V. J. (2006). The repeat domain of the melanosomal matrix protein PMEL17/GP100 is required for the formation of organellar fibers. *J Biol Chem* 281, 21198-208.
- Hoashi, T., Watabe, H., Muller, J., Yamaguchi, Y., Vieira, W. D., and Hearing, V. J. (2005). MART-1 is required for the function of the melanosomal matrix protein PMEL17/GP100 and the maturation of melanosomes. *J Biol Chem* 280, 14006-14016.
- Huizing, M., Anikster, Y., and Gahl, W. A. (2000). Hermansky-Pudlak syndrome and related disorders of organelle formation. *Traffic* 1, 823-35.
- Ito, S., and Fujita, K. (1985). Microanalysis of eumelanin and pheomelanin in hair and melanomas by chemical degradation and liquid chromatography. *Anal Biochem* 144, 527-36.
- Jimenez, M., Kameyama, K., Maloy, W. L., Tomita, Y., and Hearing, V. J. (1988). Mammalian tyrosinase: biosynthesis, processing, and modulation by melanocyte-stimulating hormone. *Proc Natl Acad Sci U S A* 85, 3830-4.
- Jimenez, M., Tsukamoto, K., and Hearing, V. J. (1991). Tyrosinases from two different loci are expressed by normal and by transformed melanocytes. *J Biol Chem* 266, 1147-56.
- Kawakami, Y., Battles, J. K., Kobayashi, T., Ennis, W., Wang, X., Tupesis, J. P., Marincola, F. M., Robbins, P. F., Hearing, V. J., Gonda, M. A., et al. (1997). Production of recombinant MART-1 proteins and specific antiMART-1 polyclonal and monoclonal antibodies: use in the characterization of the human melanoma antigen MART-1. *J Immunol Methods* 202, 13-25.
- Kawakami, Y., Eliyahu, S., Delgado, C. H., Robbins, P. F., Rivoltini, L., Topalian, S. L., Miki, T., and Rosenberg, S. A. (1994). Cloning of the gene coding for a shared human melanoma antigen recognized by autologous T cells infiltrating into tumor. *Proc Natl Acad Sci U S A* 91, 3515-3519.

- Kummer, M. P., Maruyama, H., Huelsmann, C., Baches, S., Weggen, S., and Koo, E. H. (2009). Formation of Pmel17 amyloid is regulated by juxtamembrane metalloproteinase cleavage, and the resulting C-terminal fragment is a substrate for gamma-secretase. *J Biol Chem* 284, 2296-306.
- Lavado, A., Matheu, A., Serrano, M., and Montoliu, L. (2005). A strategy to study tyrosinase transgenes in mouse melanocytes. *BMC Cell Biol* 6, 18.
- Lazova, R., Klump, V., and Pawelek, J. (2010). Autophagy in cutaneous malignant melanoma. *J Cutan Pathol* 37, 256-68.
- Lazova, R., and Pawelek, J. M. (2009). Why do melanomas get so dark? *Exp Dermatol* 18, 934-8.
- Lee, E. C., Yu, D., Martinez, D. V., Tessarollo, L., Swing, D. A., Court, D. L., Jenkins, N. A., and Copeland, N. G. (2001). A highly efficient Escherichia coli-based chromosome engineering system adapted for recombinogenic targeting and subcloning of BAC DNA. *Genomics* 73, 56-65.
- Levy, F., Muehlethaler, K., Salvi, S., Peitrequin, A. L., Lindholm, C. K., Cerottini, J. C., and Rimoldi, D. (2005). Ubiquitylation of a melanosomal protein by HECT-E3 ligases serves as sorting signal for lysosomal degradation. *Mol Biol Cell* 16, 1777-1787.
- Merillat, A. M., Charles, R. P., Porret, A., Maillard, M., Rossier, B., Beermann, F., and Hummler, E. (2009). Conditional gene targeting of the ENaC subunit genes *Scnn1b* and *Scnn1g*. *Am J Physiol Renal Physiol* 296, F249-56.
- Montoliu, L., Oetting, W. S., and Bennett, D. C. (2011). Color Genes. European Society for Pigment Cell Research. World Wide Web (URL: <http://www.espcr.org/micemut>).
- Nguyen, T., Novak, E. K., Kermani, M., Fluhr, J., Peters, L. L., Swank, R. T., and Wei, M. L. (2002). Melanosome morphologies in murine models of hermannsky-pudlak syndrome reflect blocks in organelle development. *J Invest Dermatol* 119, 1156-64.

- Plonka, P. M., Passeron, T., Brenner, M., Tobin, D. J., Shibahara, S., Thomas, A., Slominski, A., Kadekaro, A. L., HersHKovitz, D., Peters, E., et al. (2009). What are melanocytes really doing all day long...? *Exp Dermatol* 18, 799-819.
- Porret, A., Merillat, A. M., Guichard, S., Beermann, F., and Hummler, E. (2006). Tissue-specific transgenic and knockout mice. *Methods Mol Biol* 337, 185-205.
- Radtke, F., Wilson, A., Stark, G., Bauer, M., Van Meerwijk, J., Macdonald, H. R., and Aguet, M. (1999). Deficient T cell fate specification in mice with an induced inactivation of Notch1. *Immunity* 10, 547-58.
- Raposo, G., and Marks, M. S. (2007). Melanosomes--dark organelles enlighten endosomal membrane transport. *Nat Rev Mol Cell Biol* 8, 786-797.
- Rimoldi, D., Muehlethaler, K., Salvi, S., Valmori, D., Romero, P., Cerottini, J. C., and Levy, F. (2001). Subcellular localization of the melanoma-associated protein Melan-AMART-1 influences the processing of its HLA-A2-restricted epitope. *J Biol Chem* 276, 43189-43196.
- Rubera, I., Meier, E., Vuagniaux, G., Mérrillat, A.M., Beermann, F., Rossier, B.C. , and Hummler, E. (2002). A conditional allele at the mouse channel activating protease 1 (*Prss8*) gene locus. *Genesis* 32, 173-176.
- Schraermeyer, U. (1993). Does melanin turnover occur in the eyes of adult vertebrates? *Pigment Cell Res* 6, 193-204.
- Schraermeyer, U., Kopitz, J., Peters, S., Henke-Fahle, S., Blitgen-Heinecke, P., Kokkinou, D., Schwarz, T., and Bartz-Schmidt, K. U. (2006). Tyrosinase biosynthesis in adult mammalian retinal pigment epithelial cells. *Exp Eye Res* 83, 315-21.
- Smith, J. W., Koshoffer, A., Morris, R. E., and Boissy, R. E. (2005). Membranous complexes characteristic of melanocytes derived from patients with Hermansky-Pudlak

- syndrome type 1 are macroautophagosomal entities of the lysosomal compartment. *Pigment Cell Res* *18*, 417-26.
- Sviderskaya, E. V., Bennett, D. C., Ho, L., Bailin, T., Lee, S. T., and Spritz, R. A. (1997). Complementation of hypopigmentation in p-mutant (pink-eyed dilution) mouse melanocytes by normal human P cDNA, and defective complementation by OCA2 mutant sequences. *J Invest Dermatol* *108*, 30-4.
- Sviderskaya, E. V., Hill, S. P., Evans-Whipp, T. J., Chin, L., Orlow, S. J., Easty, D. J., Cheong, S. C., Beach, D., Depinho, R. A., and Bennett, D. C. (2002). p16(Ink4a) in melanocyte senescence and differentiation. *J Natl Cancer Inst* *94*, 446-54.
- Theos, A. C., Berson, J. F., Theos, S. C., Herman, K. E., Harper, D. C., Tenza, D., Sviderskaya, E. V., Lamoreux, M. L., Bennett, D. C., Raposo, G., et al. (2006). Dual loss of ER export and endocytic signals with altered melanosome morphology in the silver mutation of Pmel17. *Mol Biol Cell* *17*, 3598-612.
- Theos, A. C., Truschel, S. T., Raposo, G., and Marks, M. S. (2005). The Silver locus product Pmel17/gp100/Silv/ME20: controversial in name and in function. *Pigment Cell Res* *18*, 322-36.
- Trumpp, A., Refaeli, Y., Oskarsson, T., Gasser, S., Murphy, M., Martin, G. R., and Bishop, J. M. (2001). c-Myc regulates mammalian body size by controlling cell number but not cell size. *Nature* *414*, 768-73.
- Tsukamoto, K., Jackson, I. J., Urabe, K., Montague, P. M., and Hearing, V. J. (1992). A second tyrosinase-related protein, TRP-2, is a melanogenic enzyme termed DOPAchrome tautomerase. *EMBO J* *11*, 519-26.
- Wright, A., Kawakami, Y., and Pavan, W. (1997). Mart1 is located on mouse chromosome 19 and is excluded as a candidate for ep and ru. *Mamm Genome* *8*, 377-378.

## Figure Legends

### Figure 1. Generation of constitutive and conditional MART-1 knockout alleles

(A) Structure of the mouse *MART-1* gene locus, the targeting vector (NEO, neomycin resistance cassette, TK, thymidine kinase), the predicted targeted allele (lox-neo), the floxed allele and the knockout allele (null) (not drawn to scale). Coding exons (black boxes) 2 and 3 are located between the loxP sites, whereas exons 4 and 5 are on the targeting vector, but outside the loxP site. B, *Bam*HI. Clones that are positive for recombination on both ends were detected by PCR. The 5' external probe (probe) was used to confirm the recombined allele following *Bam*HI digestion of ES cell DNA (Figure 1B). Expected fragments of the recombined (9.5 kb) and wildtype allele (13.9 kb) are indicated. PCR primers used to distinguish the different alleles are indicated (see Materials and Methods).

(B) Southern blot analysis of double resistant ES cell clones following electroporation with the targeting vector. ES cell DNA was digested with *Bam*HI and hybridized with the 5' probe. Blots were rehybridized with a probe recognizing the neomycin resistance cassette.

(C) DNA-based PCR strategy of mice to distinguish the floxed, null and wildtype alleles.

(D) Reverse transcription-PCR (RT-PCR) analysis of RNA isolated from newborn skin demonstrates absence of *MART-1* transcripts from homozygous *MART-1*<sup>-/-</sup> mice whereas expression of *tyrosinase* and *Dct* seems not to be affected. Please note that the primers only cover the deleted region. NIH3T3, negative control, B16 mouse melanoma cells, positive control. *GAPDH* was used to control for integrity of RNA sample.

(E) Western blot of extracts from melanocytes in culture shows the absence of MART-1 protein (18 kDa) in homozygous MART-1 knockout mice.  $\alpha$ -tubulin was used to control equal loading.

(F) MART-1 expression was detected by immunostaining against MART-1 on wildtype melanocytes but not detected in MART-1 knockout melanocytes. Scale bar: 10  $\mu$ m

(G) *MART-1*<sup>-/-</sup> mice show a coat color phenotype. *MART-1*<sup>-/-</sup> mice are lighter than their *MART-1*<sup>+/-</sup> and *MART-1*<sup>+/+</sup> littermates.

**Figure 2. Melanin is reduced in *MART-1*<sup>-/-</sup> mice.**

Melanin content of 4 week-old hair (A) and eumelanin content in skin (B) samples was measured by spectrophotometry and HPLC, respectively. Hair melanin content of 19 *MART-1*<sup>+/+</sup> and 12 *MART-1*<sup>-/-</sup> samples was measured by the OD at 475nm for 1 mg hair / 1ml NaOH (\*\*\*)  $p < 0.0001$ ). Two skin samples (measurements were done in doubles) from each genotype were analyzed for eumelanin content by HPLC detection of the degradation products pyrole 2, 3, 5 tricarboxylic acid (PTCA) and pyrole 2, 3 dicarboxylic acid (PDCA).

**Figure 3. Pigment cell-specific proteins are expressed in *MART-1*<sup>-/-</sup> bulb melanocytes**

Skin sections of 1 month-old *MART-1*<sup>+/+</sup> (A-E) and *MART-1*<sup>-/-</sup> (F-J) mice were stained against tyrosinase (A, F), Tyrp1 (B, G), Dct (C, H), and Pmel17 (with  $\alpha$ Pep13h antibody – D, I and with HMB45 antibody – E, J). The images show the bulb region of the anagen hair follicles where the mature melanocytes reside. No difference was observed in distribution of pigment cell-specific proteins upon MART-1 loss. Scale bar: 10  $\mu$ m

**Figure 4. Pmel17 processing in mouse melanocytes is not affected upon MART-1 loss**

Pmel17 processing was tested by Western blot analysis. Protein extracts from *MART-1*<sup>+/+</sup> melanocyte cell line and three different *MART-1*<sup>-/-</sup> melanocyte cell lines were analyzed. melan-a cell line (mouse melanocyte) was used as a positive control and NIH3T3 cell line (mouse fibroblasts) was used as negative control. Antibody against  $\alpha$ -tubulin was used to control equal loading. Arrows indicate the corresponding fragments. Size of the protein ladder is indicated on the left.

(A) Pmel17 processing was visualized by Western blot analysis using the  $\alpha$ Pep13h antibody.  $\alpha$ Pep13h recognizes the immature P1 form and the cleavage product M $\beta$ .

(B) HMB45 antibody recognizes the M $\alpha$  and M $\alpha$ C fragments of Pmel17. Western blot against Pmel17 using HMB45 antibody showed that M $\alpha$ C fragments were produced in *MART-1*<sup>-/-</sup> melanocytes.

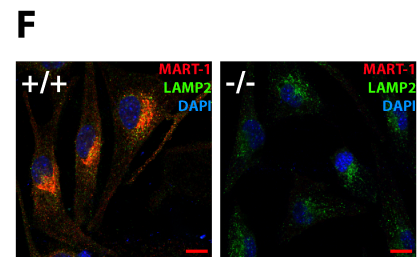
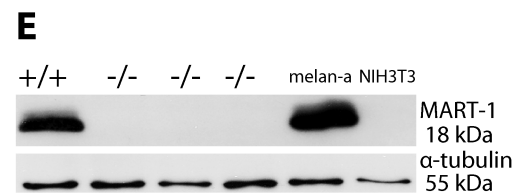
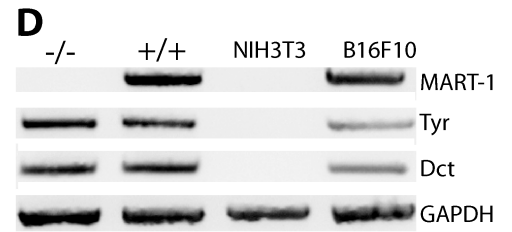
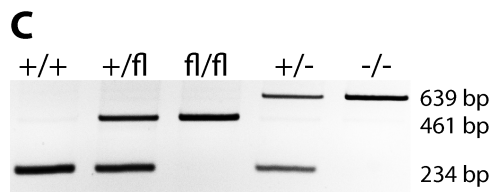
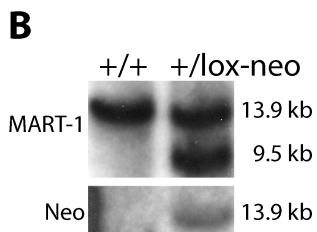
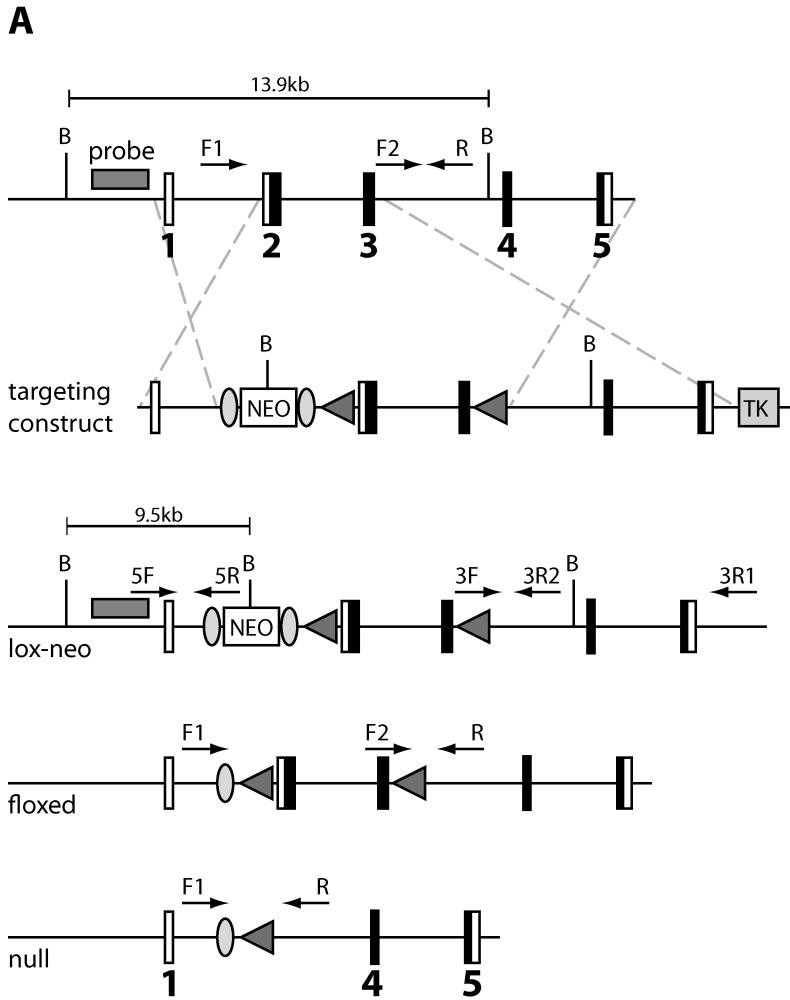
(C) The M $\alpha$ C fragments are mostly insoluble in detergents. The production of mature fibrils was detected in the insoluble protein fraction using HMB45 antibody.

(D) Pmel17 protein is processed during melanosome biogenesis. The unprocessed form is the P1 form. Arrowheads represent the proteolytic cleavage sites. The recognition sites of  $\alpha$ Pep13h and HMB45 antibodies are marked, adapted from Kummer *et al* (Kummer et al., 2009).

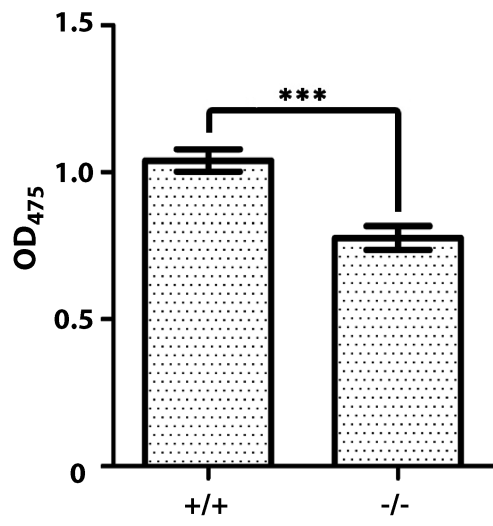
### **Figure 5. Ultrastructure of skin sections of wildtype and knockout mice reveals abnormal melanosomes**

Ultrastructure of skin samples from *MART-1*<sup>+/+</sup> (A) and *MART-1*<sup>-/-</sup> mice (B) revealed that melanosomes of hair bulb melanocytes in knockout mice were morphologically deformed. (C-G) Higher magnification micrographs of melanosomes of *MART-1* knockout mice show

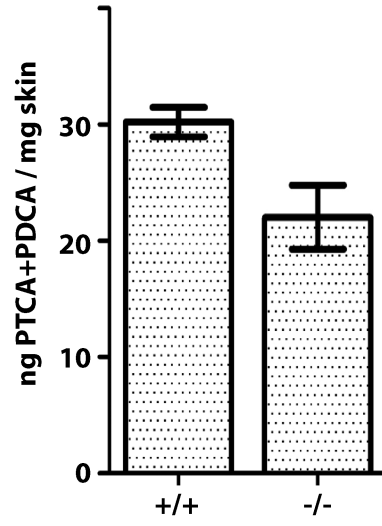
examples of blebbing of the limiting membrane and presence of presumable autophagic vesicles. (H, I) In mice carrying the classical albino mutation (*Tyrc*), melanosomes only reach immature stages I (arrows) and II (arrowheads). Ultrastructure analysis revealed no abnormalities and differences when comparing *MART-1*<sup>-/-</sup> and *MART*<sup>+/+</sup> mice on an albino (*Tyrc*) background. Scale bar: 40  $\mu$ m.

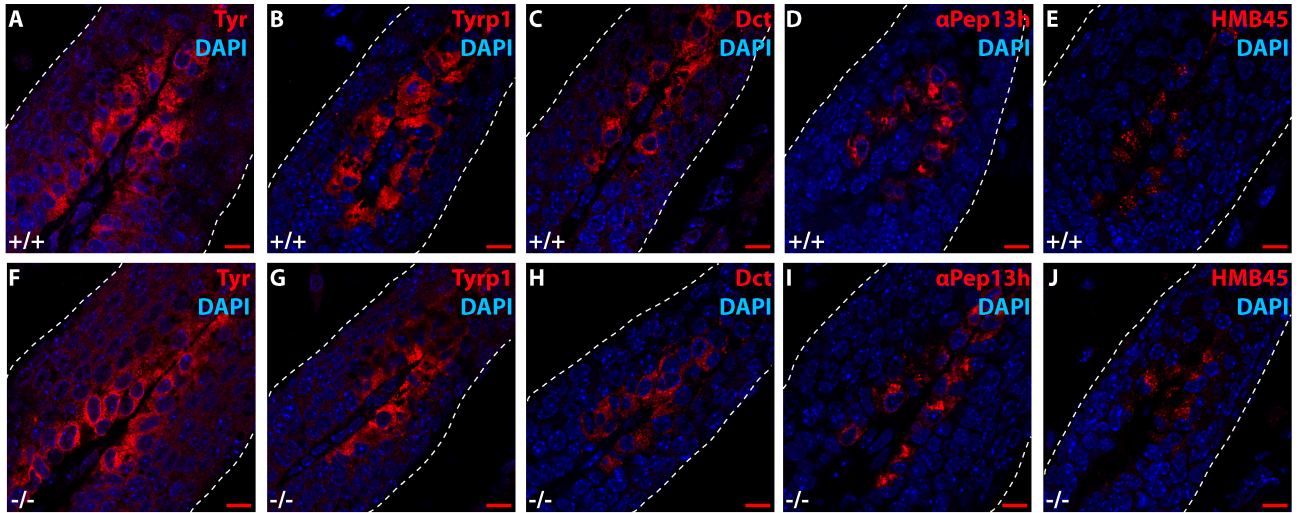


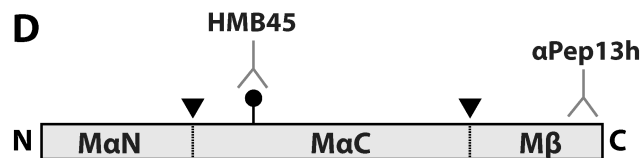
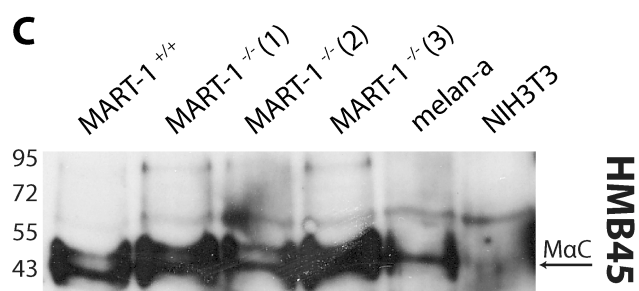
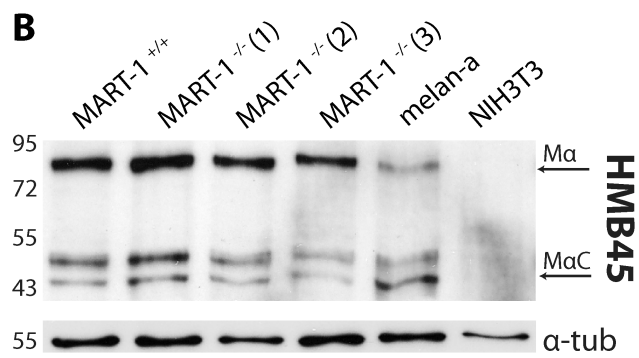
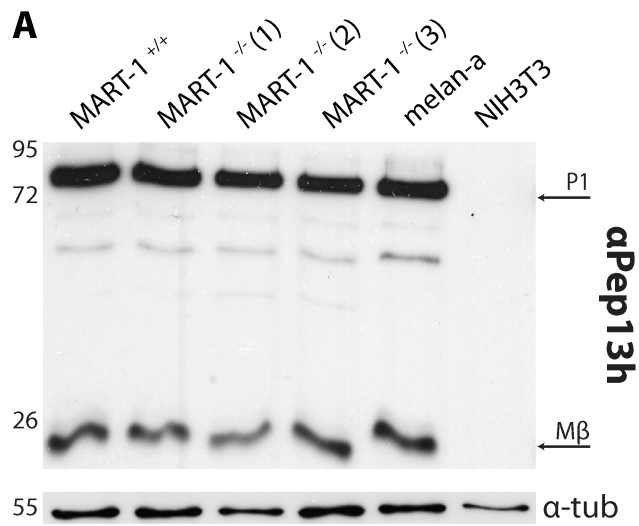
**A**

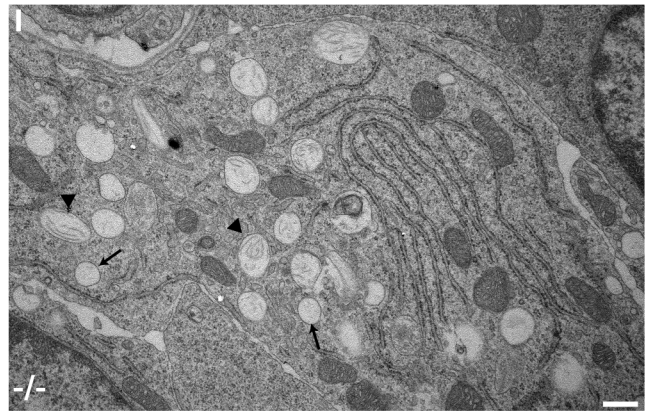
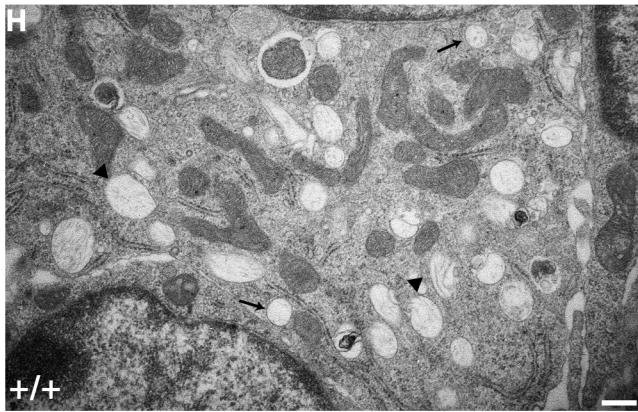
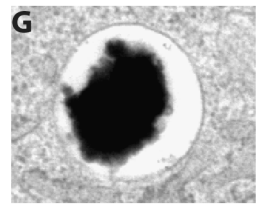
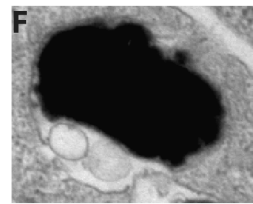
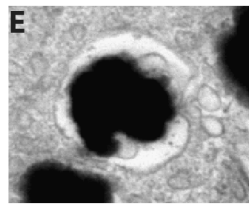
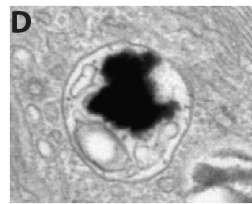
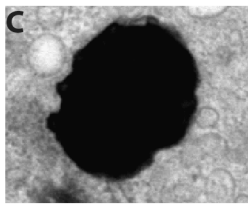
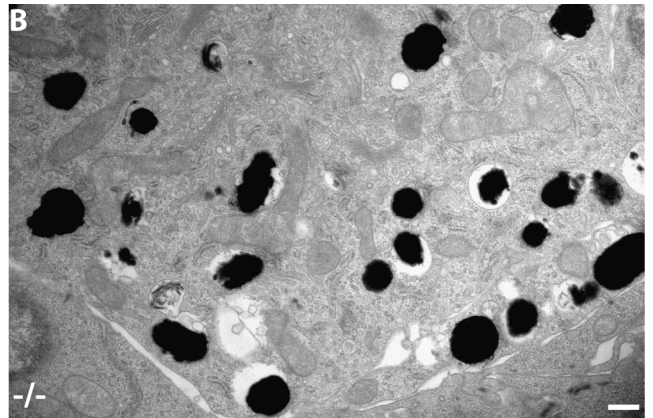
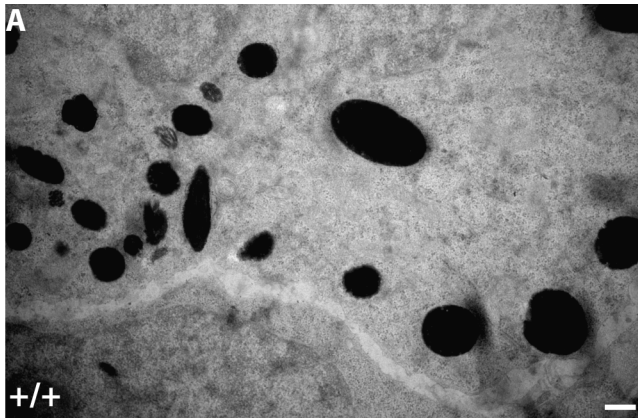


**B**









## Supplementary Figure legends

### Figure S1. Distribution of Tyrp1 and Pmel17 in wildtype and knockout melanocytes

Melanocytes extracted from *MART-1<sup>+/+</sup>* (A-B) and *MART-1<sup>-/-</sup>* (C-D) mice were cultured and stained against, Tyrp1 (A, C), and Pmel17 (B, D). In addition, the cells were co-stained against LAMP2 (a lysosomal marker). The images did not reveal any difference in subcellular distribution of Tyrp1 and Pmel17 upon MART-1 loss. In addition to these stainings, HMB45 and Pmel-N antibodies were also used to observe the distribution on Pmel17 protein in different stages of melanogenesis (not shown), and no differences were observed upon MART-1 loss. Scale bar: 10  $\mu$ m

### Figure S2. Ultrastructure of RPE layer of wildtype and knockout mice

Ultrastructure of eye samples from *MART-1<sup>+/+</sup>* (A) and *MART-1<sup>-/-</sup>* mice (B) showed that the melanosomes in the RPE cells were not affected by loss of MART-1. Scale bar: 1  $\mu$ m.

